MODELING OF SPIRAL WOUND MEMBRANE MODULE FOR CO_2 CAPTURE FROM NATURAL GAS

KHAIRIL AMRI BIN ROMLI

CHEMICAL ENGINEERING

UNIVERSITI TEKNOLOGI PETRONAS

SEPTEMBER 2015

Modeling of Spiral Wound Membrane Module for CO_2 Capture from Natural Gas

by

Khairil Amri Bin Romli
15387

Dissertation submitted in partial fulfillment of
the requirements for the
Bachelor of Engineering (Hons)
(Chemical Engineering)

September 2015

Universiti Teknologi PETRONAS,
32610, Bandar Seri Iskandar,
Perak

CERTIFICATION OF APPROVAL

Modeling of Spiral Wound Membrane Module for CO_2 Capture from Natural Gas

by

Khairil Amri Bin Romli
15387

A project dissertation submitted to the
Chemical Engineering Programme
Universiti Teknologi PETRONAS
in partial fulfillment of the requirements for the
BACHELOR OF ENGINEERING (Hons)
(CHEMICAL ENGINEERING)

Approved by,

_____
(Dr Lau Kok Keong)

UNIVERSITI TEKNOLOGI PETRONAS
BANDAR SERI ISKANDAR, PERAK
September 2015

CERTIFICATION OF ORIGINALITY

This is to certify that I am responsible for the work submitted in this project, that the original work is my own except as specified in the references and acknowledgements, and that the original work contain herein have not been undertaken or done by unspecified sources or persons.

_____

KHAIRIL AMRI BIN ROMLI

ABSTRACT

The search for viable alternatives to the traditional energy intensive techniques method such as distillation and adsorption has led to the massive research on membranes. Fiber tube membrane module and spiral wound membrane module (SWM) emerged as the most widely used in industry compared to other membrane module due to their high mass transfer area. However, fiber tube module has been dominating in the gas separation industry including the capture of CO_2 from natural gas while spiral wound module is used widely in reverse osmosis application. Hence, this thesis aims to overcome the limitation of the available literature for mathematical modeling of spiral wound module for gas separation. A new approach to solve the mass transfer problem posed by the permeation in spiral wound module is presented. A two dimensional mass transfer in a radial crossflow has been modeled using 'succession of state' approach. The algorithm models the spiral wound module separation for CO_2 capture from natural gas, simulating the permeate and residue composition as well as the flow rate in MATLAB. Several factors including feed flow rate, feed pressure and leaf number are proved to affect the performance of spiral wound module.

ACKNOWLEDGEMENT

First and foremost, I am grateful to God for the good health and wellbeing that were necessary to complete this thesis.

I would like to express my special appreciation and thanks to my supervisor, Dr. Lau Kok Keong, who have been a tremendous mentor for me. He continually gives me his full support during the entire eight months of Final Year Project. Without his supervision and constant help this project would not have been possible.

I would also like to thank Serene Sow Mun Lock who was always ready to share her knowledge and information regarding membrane separation with me. The information has been crucial in helping me completing this thesis. I would like to extend my gratitude to Dr. Nurul Ekmi Binti Rabat, the coordinator for Final Year Project II who is so supportive during the completion of this thesis.

A special thanks to my family. Words cannot express how grateful I am to them for all of the sacrifices that they've made on my behalf. Their prayer for me was what sustained me thus far. I would also like to thank all of my friends who supported and incented me to strive towards my goal.

TABLE OF CONTENTS

CERTIFICATION ii

ABSTRACT iv

ACKNOWLEDGEMENT v

TABLE OF CONTENTS vi

LIST OF FIGURES viii

LIST OF TABLES ix

LIST OF ABBREVIATIONS ix

CHAPTER 1: INTRODUCTION 1

1.1 Background of study 1

1.2 Problem Statement 3

1.3 Objectives 4

1.4 Scope of Study 4

CHAPTER 2: LITERATURE REVIEW 6

2.1 Membrane modules 6

2.1.1 Tubular module 6

2.1.2 Plate and frame module 7

2.1.3 Hollow fiber tube 7

2.1.4 Spiral wound module 8

2.2 Spiral wound module configuration 9

2.2.1 Permeate spacer 9

2.2.2 Feed spacer 9

2.2.3 Permeate tube 10

2.3 Concentration polarization 10

2.4 Literatures on membrane modules for gas separation 10

2.5 Research gap 13

CHAPTER 3: METHODOLOGY 15
3.1 Model development 15
3.2 Local permeation rate 16
3.3 Radial crossflow 17
3.4 Algorithm for the model 18
3.5 Simulation method 21
3.6 Gantt Chart and milestones 22

CHAPTER 4: RESULT AND DISCUSSION 23
4.1 Simulation result 23
4.2 Model validation 26
4.3 The effect of feed flow rate 29
4.4 The effect of feed pressure 30
4.5 The effect of membrane leaf number 32

CHAPTER 5: CONCLUSION AND RECOMMENDATION 34
5.1 Conclusion 34
5.2 Recommendation 35

REEFERENCES 36

APPENDICES 40

LIST OF FIGURES

Figure 1.1:	A schematic view of a spiral wound membrane module (Johnson and Busch, 2010)	5
Figure 2.1:	Tubular module (Mulder, 1996)	6
Figure 2.2:	Plate and frame module (Baker, 2000)	7
Figure 2.3:	Hollow fiber module for bore-side feed (Baker, 2000)	7
Figure 2.4:	Spiral wound module (Mulder, 1996)	8
Figure 3.1:	Radial crossflow permeator	17
Figure 3.2:	Schematic algorithm of SWM elements	18
Figure 3.3:	Gantt Chart and key milestones	22
Figure 4.1:	CO_2 permeate composition profile in radial direction	24
Figure 4.2:	CO_2 permeate flow rate profile in radial direction	24
Figure 4.3:	CO_2 retentate composition profile in axial direction	25
Figure 4.4:	CO_2 retentate flow rate profile in axial direction	25
Figure 4.5:	Model validation with published experimental data of CO_2 permeate composition	27
Figure 4.6:	Model validation with published experimental data of stage cut	28
Figure 4.7:	Effect of feed flow rate on CO_2 permeate composition along active membrane length	29
Figure 4.8:	Effect of feed flow rate on CO_2 permeate flow rate along active membrane length	30
Figure 4.9:	Effect of feed pressure on CO_2 permeate composition along active membrane length	31
Figure 4.10:	Effect of feed pressure on CO_2 permeate flow rate along active membrane length	31
Figure 4.11:	Effect of number of leaf on CO_2 permeate composition along active membrane length	32
Figure 4.12:	Effect of number of leaf on CO_2 permeate flow rate along active membrane length	33

LIST OF TABLES

Table 1.1: Principal gas separation markets, producers, and membrane systems (Baker, 2002) 3

Table 2.1: Summary of literature regarding membrane module for gas separation 14

Table 3.1: Input parameters used for the simulation of a case study within MATLAB (S.S.M. Lock et al., 2015) 21

Table 4.1: Experiment data from Qi and Henson (1996) 26

Table 4.2: Comparison of experiment data and simulation result for CO_2 permeate composition, y_p 27

Table 4.3: Comparison of experiment data and simulation result for stage cut 28

LIST OF ABBREVIATIONS

List of symbols

i	index (varies in axial direction)
j	index (varies in radial direction)
k	index for number of leaf
P_1	permeability of carbon dioxide
P_2	permeability of methane
p_H	pressure in feed side
p_L	pressure in permeate side
Q_P	permeate flow rate
Q_R	retentate flow rate
x_1	composition of carbon dioxide in the retentate
x_2	composition of methane in the retentate
y_1	composition of carbon dioxide in the permeate
y_2	composition of methane in the permeate

Greek symbols

ΔQ	total flow rate permeation into an element
ΔQ_1	flow rate permeation of carbon dioxide into an element

α	ideal permeability of CO_2/CH_4
β	ration of pressure on feed side to permeate side
δ	thickness of active layer on membrane
θ	stage cut

CHAPTER 1

INTRODUCTION

1.1 Background of Study

During the 19th century, the unwanted natural gas was a disposal problem in the active oil field. Natural gas (NG) was burned off at the oil fields because it was considered as the byproduct of the producing oil. However, the demand for natural gas has been increasing vastly nowadays and is considered as the world safest, cleanest and most efficient energy sources (Schoots et al., 2011; Speight, 2007; Xiao et al., 2009). In addition, natural gas is the fastest growing primary source of energy in the current global economy (Kidnay et al., 2011; Mokhatab et al., 2006; Nord et al., 2009; Speight, 2007). Natural gas is primarily consists of methane (CH_4). Besides that, NG contains certain composition of heavier gaseous hydrocarbons, acid gases, water vapors, mercury, radioactive gases and other gases such as carbon dioxide, nitrogen and helium (Yergin, 2011). The combustion of natural gas emits approximately 26% of carbon dioxide (CO_2) which is 41% lower CO_2 emission factor than coal and oil (Armaroli and Balzani, 2011).

According to the fourth assessment report of the United Nations Intergovernmental Panel on Climate, the increasing amount of CO_2 in the atmosphere will contribute to greater greenhouse effect and consequently can cause climate change (IPCC, 2007). Other studies revealed that 60% of greenhouse gases is CO_2 (Shao et al., 2013). In order to mitigate the climate change effect, oil and gas companies are urged to implement practices which reduce CO_2 composition in NG processing (Gnanendran and Hart, 2009). Hence, a standard that specify the pipeline for CO_2 in NG to operate below 2% is implemented (Baker and Lokhandwala,

2008). This enforcement stresses the requirement to capture CO_2 in the industrial application (Baker and Lokhandwala, 2008). CO_2 capture will also enhance the calorific value of natural gas, decrease the gas volume transports trough pipeline and cylinders and reduce pipeline corrosion (Chew et al., 2010; Mokhatab et al., 2006; Ren et al., 2002; Xiao et al., 2009).

Adsorption, cryogenic distillation and membrane separation are commonly used in CO_2 capture or removal (Ahmad et al., 2008a,b, 2009; Chew et al., 2010; Kidnay et al., 2011; Meindersma and Kuczynski, 1996). Among those separation techniques, the most developed commercial technology is amine absorption. However, high energy consumption for solvent regeneration, equipment corrosion, and flow problems caused by changes in viscosity are some of the disadvantages which discouraging its continued usage (Ahmad et al., 2008b; Chew et al., 2010; Merkel et al., 2001; Ohlrogge et al., 2002). So, other technology which is cheaper and energy efficient such as membrane separation is being researched and developed heavily. Membrane able to yield higher separation efficiency in faster separation using the compact modules while very space effective which differentiate membrane gas separation from other separation technique for industrial application (Baker and Lokhandwala, 2008; Cao et al., 2002; Ng et al., 2004; Reijerkerk et al., 2011a; Zhao et al., 2006).

Hollow fiber modules and spiral wound modules offer much larger mass transfer areas than the other modules which explain their domination in most commercial membrane processes (Bhattacharyya et al., 1992). However, most of today's gas separation membranes are formed into hollow fiber modules, with perhaps fewer than 20% being formed into spiral-wound modules (Baker, 2002). Despite that, the ease of flat membrane preparation, low pressure build-up of the permeate stream, and low pressure loss of the feed stream increase the popularity of spiral wound membranes in the current separator designs (Koros and Chern, 1987; Baker, 2002). Table 1.1 illustrates the popularity of membrane modules used in the industry.

Table 1.1: Principal gas separation markets, producers, and membrane systems (Baker, 2002)

Company	Principal markets/ estimated annual sales	Principal membrane material used	Module type
GMS (Kvaerner) Separex (UOP) Cynara (Natco)	Mostly natural gas separations Carbon dioxide/methane ($30 million/year)	Cellulose acetate	Spiral-wound Hollow fiber
Permea (Air Products) Medal (Air Liquide) IMS (Praxair) Generon (MG)	Large gas companies Nitrogen/Air ($75 million/year) Hydrogen separation ($25 million/year)	Polysulfone Polyimide/polyaramide Polyimide Tetrabromo polycarbonate	Hollow fiber
Aquilo Parker-Hannifin Ube GKSS Licensees MTR	Vapor/gas separation, air dehydration, other ($20 million/year)	Polyphenylene oxide Polyimide Silicone rubber	Hollow fiber Plate-and-frame

1.2 Problem Statement

The application of spiral wound membrane module (SWM) in gas separation process is receiving less popularity if compared to hollow fiber module despite of its huge advantages in separation process. SWM demonstrates good control of concentration polarization and fouling, moderate permeate side pressure drop and suitable for high pressure operation. Hence, these advantages should provide SWM a huge opportunity to begin dominating the gas separation process in the coming years provided with enormous amount of literature study and mathematical model for spiral wound module.

Spiral wound module is used most widely in particles-liquid separation especially for the new reverse osmosis system. Hence, there are many mathematical models developed for SWM regarding particle-liquid separation. On the other hand, the mathematical model available for SWM in gas separation is limited due to the less popularity in the current commercial application.

The mathematical modeling for membrane gas separators was first issued by Weller and Steiner (1950). Since then, various models for gas separation permeators have been proposed in the literature. Various mathematical models and calculation methods for the symmetric membranes and high-flux asymmetric membranes have

been reported in the literature with different flow and module configurations. However, most of the developed mathematical model for gas membrane separation is related to hollow fiber module. Since there is limited mathematical model available for membrane wound membrane module, it is crucial to develop a mathematical model for SWM in order to predict the separation performance of SWM.

1.3 Objectives

In summary, this project is concerned with the development of tools that help to understand and design spiral wound module. The objectives of this study are:

1. To develop of a mathematical model for spiral wound membrane module for gas separation.
2. To evaluate the separation performance for spiral wound module under different sensitivity analysis using the developed mathematical model.

1.4 Scopes of Study

This project focuses on spiral wound membrane module as the method for membrane gas separation. Another membrane module which is used widely in the gas industry is hollow fiber membrane. These two are the most commercially used in the industry due to their high packing density, which allowing maximum area separation over volume required (Bhattacharyya et at., 1992).

The modules of spiral wound are made of flat membrane envelopes or leaf, wrapped around a central tube. Feed passes along the length of the module and the permeate passes into a membrane leaf and then out via the central tube. A membrane leaf typically consists of two membrane sheets separated by a spacer sheet form the channel for feed or permeate flow. Modern spiral wound module tends to contain multiples envelop/leaf that are all attached to the same central tube. A typical spiral wound module is shown schematically in Fig. 1.1.

A new approach to model the separation of spiral wound module is developed in this study. The developed mathematical model is used in the simulation

by using a case study for CO_2 capture from natural gas. The evaluation for separation performance of spiral wound module considers the effect of feed flow rate, feed pressure and membrane leaf. Other effects such as concentration polarization and pressure drop in feed and permeate spacer are not included in this study.

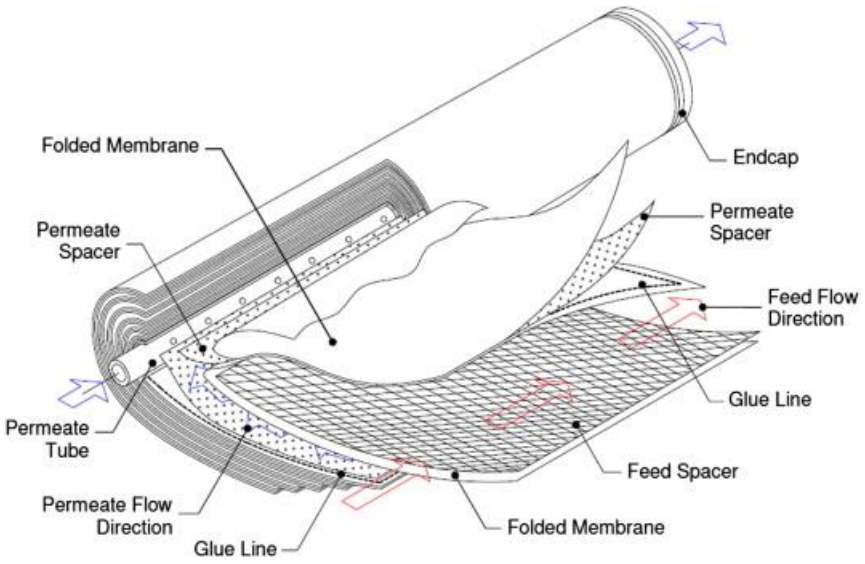

Figure 1.1: A schematic view of a spiral wound membrane module (Johnson and Busch, 2010)

CHAPTER 2

LITERATURE REVIEW

2.1 Membrane Modules

Commercial separation demand efficient mass transfer in order to minimize cost and plant size. Hence, a large membrane area needs to be tightly packaged into membrane modules. Several membrane modules which display different membrane geometry have been developed for this purpose. The modules must be able to provide large membrane area per unit volume. The most commonly used membrane modules are tubular modules, plate and frame modules, hollow fiber modules and spiral wound modules. As hollow fiber modules and spiral wound modules offer much large mass transfer areas than the other two modules, they dominate most commercial membrane processes, accounting for all new reverse osmosis system (Bhattacharyya et at., 1992).

2.1.1 Tubular Module

Tubular membrane units are supported on the inside of porous pressure tight tubes (12 to 25 mm in diameter). Feed is passed through inside of the membrane tubes. Even though the mass transfer area are not as large as in spiral-wound and hollow fiber membranes, tubular membranes are less susceptible to fouling and are easier to clean compared to those modules (Brouckaert and Buckley, 1992).

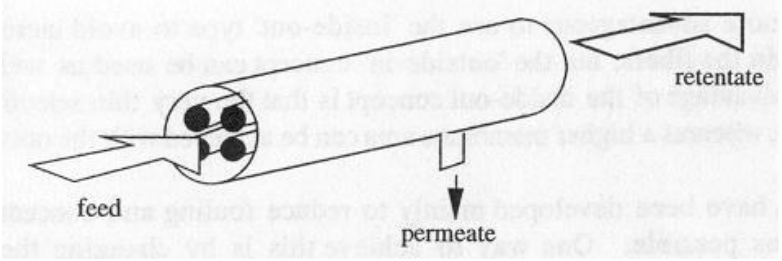

Figure 2.1: Tubular module (Mulder, 1996)

2.1.2 Plate and Frame Module

Plate and frame module is the simples and most robust module compared to the other modules. The feed flows in flat channel between the two membranes which are placed one on top of another. Packing densities for this module vary from 100 to 400 m^2/m^3 (Marriott et al., 2001). Plate and frame module is commonly used for pervaporation.

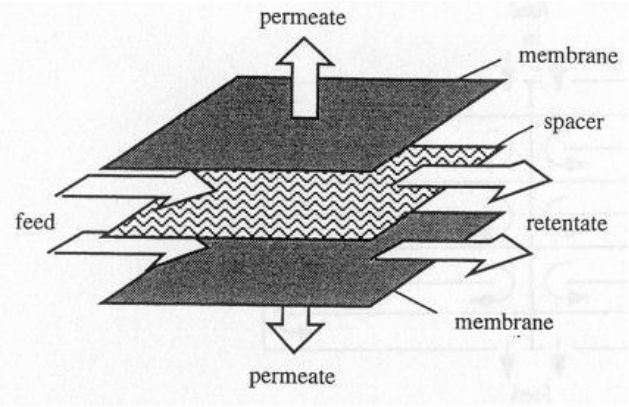

Figure 2.2: Plate and frame module (Baker, 2000)

2.1.3 Hollow Fiber Module

In hollow fiber module, a large number of membranes tubes are packed into a module shell. The small diameter of the fibers causes this configuration to pack in high density. In addition, hollow fiber module is difficult to clean. On the other hand, its membrane permeability is usually lower than spiral wound module (Bhattacharyya et al., 1992).

Generally, feed is introduced outside the hollow fiber with material permeating into the interior part. The feed mixture may flow through the fiber bundle radially or parallel to the hollow fibers. On the other hand, for gas separation counter-current flow modules are generally used, whereas the cross-flow pattern seen in radial flow modules is preferred for reverse osmosis (Narinsky, 1991).

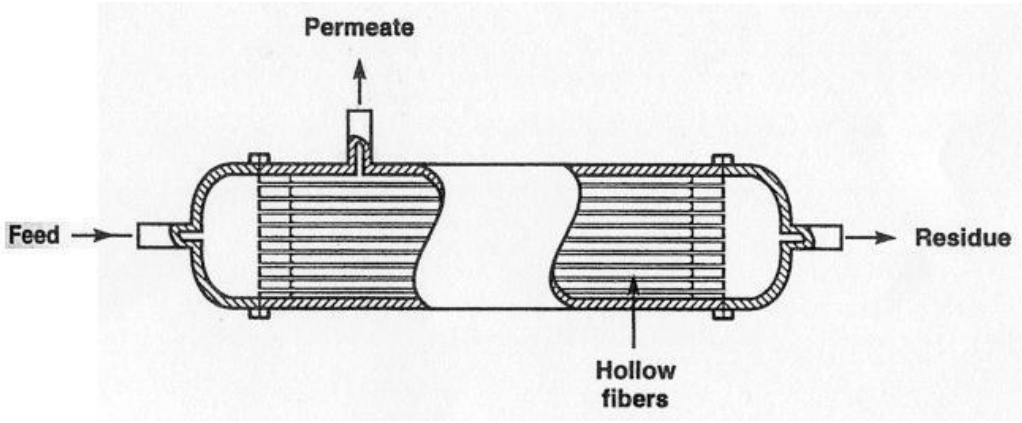

Figure 2.3: Hollow fiber module for bore-side feed (Baker, 2000)

2.1.4 Spiral Wound Module

Spiral wound module is flat membrane sheets separated by highly porous spacer material. The modules are relatively simple to build and have a high packing density (> 900m^2 /m^3), but are difficult to clean (Marriott et. al., 2001). A typical SWM module is schematically shown in the figure below. A membrane envelope is made of two sheets, glued at the three edges, with a fabric filling the permeate channel. The open permeate-side of this envelope is fixed on a perforated inner tube (permeate collector tube) where permeate is collected. Several envelopes, separated by relatively thin net-type spacers, are tightly wrapped around the perforated inner tube. The feed flows parallel to the central tube outside the membrane envelopes (axially). Material permeates into the interior of the membrane envelopes and flows along the spiral, towards the central tube (radially). The modules are almost always operated with a cross-current flow pattern.

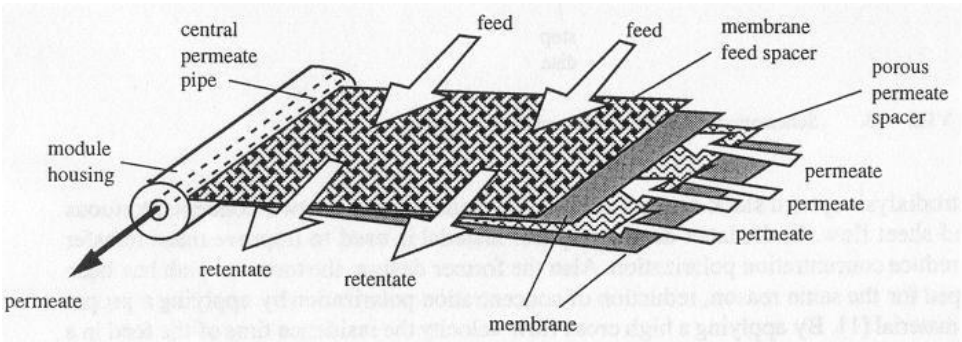

Figure 2.4: Spiral wound module (Mulder, 1996)

2.2 Spiral Wound Module Configuration

Spiral wound membrane (SWM) envelope consists of two flat sheet membranes which are glued on three edges of a permeate spacer. The fourth open edge is attached to the perforated permeate tube. A feed spacer is placed on either side of the membrane envelope and wounded with the membrane leaf around the central tube. On the other hand, a permeate spacer is a material which create the permeate channel in the membrane envelope and direct the liquid flow of permeate solution to the permeate tube.

2.2.1 Permeate Spacer

The permeate spacer is a sheet of material placed between the backsides of the membrane to form a membrane envelope. It promotes the flow of permeate towards the center tube for discharge. The permeate spacer material must be able to withstand the pressure of operation without collapsing and blocking the flow. In addition, its surface must smooth to prevent intrusion of the membrane backing material into the permeate spacer. A polyester knit tricot stiffened with polymeric materials is commonly used for normal operating pressures up to 600 psi (40.8 bar). Combinations of tricot and other polymeric materials which are stronger are used for operating pressure more than 600 psi (Marriott et. al., 2001).

2.2.2 Feed Spacer

Feed spacer plays a major role regarding the mass transfer, homogenizing and mixing behavior in membrane separation. In spiral wound modules, feed spacers are introduced to develop feed channel, by keeping the membrane surfaces apart. Presence of feed spacers generate secondary flow patterns within the membrane module which may lead to enhance mass transport of the solute away from the membrane to minimize concentration polarization, which is a desirable feature for efficient membrane operations. However, the undesirable features associated with their use are increased pressure drop and development of fluid stagnant zones. Therefore, the efficiency of a membrane module depends largely on the efficacy of

the spacers to increase mass transport away from the membrane surface into the bulk fluid at moderate pressure loss. The geometries and configuration of the feed spacer determine its suitability and performance in particular applications. Diamond pattern spacer, parallel pattern spacer and corrugated pattern spacer are commonly used in industry.

2.2.3 Permeate Collector Tube

The permeate tube is the center of the element which membrane leaves, permeate spacer and feed spacer are wound. Known as center tube, permeate tube is perforated to allow the permeate flow spirally through the permeate spacer to the center of the element. The center tube also provides the overall structural strength to the module.

2.3 Concentration Polarization

When a mixture passes through a membrane, there will usually be a buildup of the slower penetrant towards the interface and a depletion of the faster penetrant. This is referred to as concentration polarization. Excessive concentration polarization not only retards the productivity of a membrane plant, it can also cause precipitation (scaling) and thus reduce the life of the membrane. Although the effect of concentration polarization on the overall mass transfer coefficient in gas systems is usually negligible (Mulder, 1996; Narinsky, 1991), it can have a considerable effect on the overall resistance in solvent systems such as reverse osmosis.

2.4 Literatures on Mathematical Model for Membrane Modules Used for Gas Separation

Pan (1983) studied a mathematical model to examine the performance of a permeator with asymmetric membrane for a binary gas mixture. The model considered the permeate pressure drop and was applicable to both hollow-fiber and spiral wound modules. The effect of permeate-feed flow pattern on module

performance was analyzed. The mathematical model was verified by large-scale pilot-plant experiments for helium recovery from natural gas using large hollow-fiber module.

Chern et al. (1985) developed a model for simulating the performance of an isothermal hollow-fiber gas separator for binary gas mixtures. The model took into account permeate pressure build-up and concentration dependence of the permeability by using the dual-mode sorption and transport models. The effects of possible penetrant competition according to the generalized dual-mode model were examined. They presented the effects on separator performance caused by changes in fiber dimensions, feed pressure, membrane area, feed composition, and feed flow rate. They discussed about a triple-separator arrangement for the separation of a 12%/88% CO_2/CH_4 mixture to illustrate how the results of single-stage studies could be readily extended to multistage design consideration. Direct experimental verification had not been reported.

Runhong and Michael (1996) produced an approximate modeling technique for spiral-wound permeator separating binary gas mixtures. They derived the mathematical model directly from a standard fundamental model developed by Pam (1983). They also assumed the residue flow rate to be constant in the direction of permeate flow. This assumption reduces the original boundary value problem to a more computationally tractable problem involving a small number of nonlinear algebraic equations. Theoretical justification for the modeling technique is obtained via comparison to one-point collocation. The approximate modeling and parameter estimation techniques are evaluated for the separation of CO_2/CH_4 mixtures.

Thundyil and Koros (1997) presented and analyzed theoretically a new approach to solve the mass transfer problem posed by the permeation process in a hollow fiber permeator for radial crossflow, countercurrent, and co-current flow patterns. They dealt with binary separations. The new approach based on finite element was named as “Succession of States method”. Although they claimed that this approach can easily handle incorporation of pressure, composition and temperature dependent permeability, there was no experimental validation.

Coker et al. (1998) developed a model for multicomponent gas separation using a hollow-fiber contactor which permits simulation of co-current,

countercurrent, and cross-flow contacting patterns with permeate purging (or sweep). They followed a stage-wise approach to convert the differential equations to a set of coupled, non-linear differential equations. Although they claimed that their methodology could easily incorporate pressure dependence permeability, they assumed constant permeability in their modeling work. Model validation had not been verified with experimental data.

Marriott et al. (2001) presented another detailed mathematical model of membrane modules for multicomponent gas separation based on rigorous mass, momentum and energy balances, and the orthogonal collocation was the preferred method for solving the partial differential and algebraic equations. The main drawback of this model is that it needs the knowledge of molecular diffusivity and solubility (both are difficult to measure) instead of the permeability. This is especially the case when asymmetric composite membranes are used. Consequently, the applicability of the model is constrained by the uncertainty in getting such parameters required by the model. Marriot and Sørensen (2003a) extended the work of Marriott et al. (2001) to model also spiral-wound membrane module by following a general approach.

Wang et al. (2002) studied the CO_2/CH_4 mixed gas permeation through hollow fiber membranes permeator. An approach to characterize the true separation performance of hollow fiber membranes for binary gas mixtures was provided based on experiments and simulations. The influences of pressure drop within the hollow fibers, non-ideal gas behavior in the mixture and concentration polarization were taken into consideration in the mathematical model. They obtained calculated CO_2 permeance in a mixed gas permeator close to that obtained in the pure gas tests and they attributed this to the net influence of the non-ideal gas behavior, competitive sorption and plasticization. The CH_4 permeance was higher in the mixed gas tests than that in the pure gas tests, as the plasticization caused by CO_2 dominated the permeation process.

Miki and Kenji (2010) studied the permeation properties of single and binary CO_2/CH_4 mixture using a module of carbon hollow fiber membranes derived from sulfonated poly(phenylene oxide) (SPPO). They managed to investigate the required SPPO carbon membrane pore size distribution that demonstrates high CO_2/CH_4

selectivity for single and binary gas separation. Moreover, they studied the effect of permeation temperature, total feed pressure and CO_2 feed concentration on separation performances of the carbon hollow fiber membrane module.

Faizan et al. (2014) developed a mathematical model dealing with the hollow fiber module characteristics that can be included within a commercial process simulator for gas separation system. In their study, a hollow fiber membrane model was incorporated in Aspen HYSYS to simulate the separation of carbon dioxide and methane. They studied a double stage module with a permeate cycle with considering the important of fiber length, radius of the fiber bundle, diameter of the fibers and porosity on the separation performance and economics perspective. Furthermore, the hollow fiber membrane model was verified experimentally. Table 2.1 summarizes the above literatures regarding membrane module for gas separation.

2.5 Research Gap

Table 2.1 shows the summary of several available literatures of membrane modules for gas separation from early 80's until the recent years. Most of the literatures produced were related to hollow fiber module. On the other hand, the available literatures on spiral wound module are so limited when compared to hollow fiber. In addition, simulation is one of the fast routes to determine the performance of spiral wound module separation other than conducting experiment. Hence, the development of mathematical modeling for SWM is important to be applied in the simulation phase.

Table 2.1: Summary of literature regarding membrane module for gas separation

Author	Year	Tittle	Related Membrane Module
Pan	1983	Gas separation by permeators with high flux asymmetric membranes	Hollow fiber Spiral wound
Chern et al.	1985	Simulation of a hollow-fiber gas separator: the effects of process and design variables	Hollow fiber
Runhong and Michael	1996	Optimal design of spiral-wound membrane networks for gas separations	Spiral wound
Thundyil and Koros	1997	Mathematical modeling of gas separation permeators – for radial crossflow, countercurrent, and cocurrent hollow fiber membrane modules	Hollow fiber
Coker et al.	1998	Modeling multicomponent gas separation using hollow-fiber membrane contactors	Hollow fiber
Marriott et al.	2001	Detailed mathematical modeling of membrane modules	Spiral wound Hollow fiber
Wang et al.	2002	Characterization of hollow fiber membranes in a permeator using binary gas mixtures	Hollow fiber
Miki and Kenji	2010	CO_2/CH_4 Mixed Gas Separation Using Carbon Hollow Fiber Membranes	Hollow fiber
Faizan et al.	2014	Hollow fiber membrane model for gas separation: Process simulation, experimental validation and module characteristics study	Hollow fiber

CHAPTER 3

METHODOLOGY

3.1 Model development

The mathematical model involved in the application of succession of states method which is adapted from Thundyil and Koros (1997) reduces the problem to a number of finite elements or cells where each cell is considered to be independent to one another. Lock et al. (2015) highlighted that the outlet condition of one cell is computed based on the specified inlet condition provided and will be the inlet condition of the subsequent cell. The model is only completed when the computation is performed over the entire membrane module cells.

The computation of the binary CO_2/CH_4 separation within spiral wound membrane module requires the following input for calculating the mass balance from one cell to the subsequent cell:

a) Membrane characteristic:
    i. Gas permeance of CO_2 and CH_4 in the feed
    ii. Thickness of active layer on membrane
b) Feed gas characteristic:
    i. Feed composition
    ii. Feed pressure
    iii. Feed flow rate
c) Membrane module characteristic
    i. Active area of membrane module
    ii. Active length of permeate tube collector

3.2 Local Permeation Rate

The solution diffusion model is the most widely accepted transport mechanism for gas separation through membranes. Faizan et al. (2014) stated that the transport mechanism consists of three steps:

i. The sorption of feed gas molecules into the membrane interface
ii. Diffusion through the complete membrane thickness
iii. Desorption of the absorbed gas on the permeate side.

The governing flux equation is given by Fick's Law of diffusion where the driving force is the partial pressure difference across the membrane:

$$J_i = \frac{P_1}{\delta}(p_H x_i - p_L y_i) \tag{1}$$

where J_i is the flux of the gas component, p_H and p_L are the feed and permeate side pressures, respectively, x_i and y_i are the fractions of component i on the feed and permeate sides, respectively, and δ is the membrane thickness.

For the binary gas mixture, the permeation rate at any point on a differential membrane area, dAm can be expressed as:

$$ydV = \frac{P_1}{\delta}[p_H x - p_L y]dA_m \tag{2}$$

$$(1-y)dV = \frac{P_2}{\delta}[p_H(1-x) - p_L(1-y)]dA_m \tag{3}$$

By dividing equation (2) by (3), the following is obtained:

$$\frac{y}{1-y} = \frac{\alpha\left[x - \left(\frac{p_L}{p_H}\right)y\right]}{(1-x) - \left(\frac{p_L}{p_H}\right)(1-y)} \tag{4}$$

where P_1 and P_2 represent the permeability of the pure gas component which are CO_2 and CH_4. x and y are the feed and permeate composition at any point along the membrane. δ is the thickness of active membrane layer and α represents the membrane selectivity given by:

$$\alpha_{ij} = \frac{P_1}{P_2} \tag{5}$$

3.3 Radial Crossflow

The radial crossflow permeator is schematically represented in Figure 3.1. In the radial crossflow, the incoming gas feed flows through the membrane and generates two outlet streams which are called as retentate and permeate. The gas permeation flow radially inward perpendicular to the feed channel towards the permeate collector tube. On the other hand, the retentate stream is the residue of feed stream which flows axially along the permeate collector tube.

Many conditions may vary within the system. For example, there will be a pressure drop in the feed channel and the permeability of the membrane to components which is a function of composition, pressure and temperature may vary along the membrane. However, these factors are sufficiently constant to neglect their variation in modelling (Thundyil and Koros, 1997). The following assumptions are made for the ease of the mathematical modelling:

a. Negligible pressure variation in feed and permeate spacer.
b. Permeability of gases is independent of pressure, temperature and concentration.
c. Neglect the curvature of the channel by considering the membrane leaf as a flat channel.

Given the assumptions above and considering that the feed only move axially to the permeate collector tube while the permeate only move radially inward, the flow is characterized a two-dimensional model.

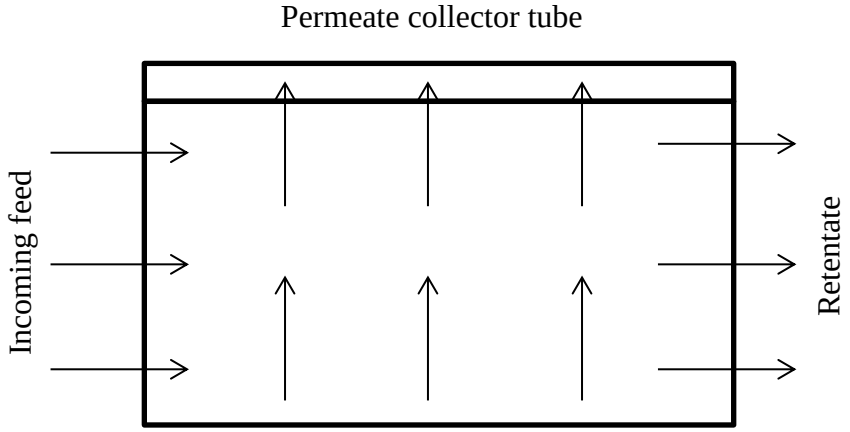

Figure 3.1: Radial crossflow permeator

3.4 Algorithm for the Model

The algorithm starts at the feed end for the first element on the first leaf of the membrane module. The mass transfer across the membrane for the first element/cell is computed before proceeding to the next element. A schematic representation of the approach is illustrated in Figure 3.2. There are four types of elements (Types I and II, and Types III and IV) in the case of radial crossflow, where the mass transfer computations are different.

The various elements are shown in their relative radial and axial locations. The computation proceeds radially from the Type I element to a succession of Type II elements and finally proceeds into the permeate collector tube. Then it starts again radially to the permeate collector tube from a Type III element through a succession of Type IV elements. The successive axial steps are taken to the residue stream (retentate).

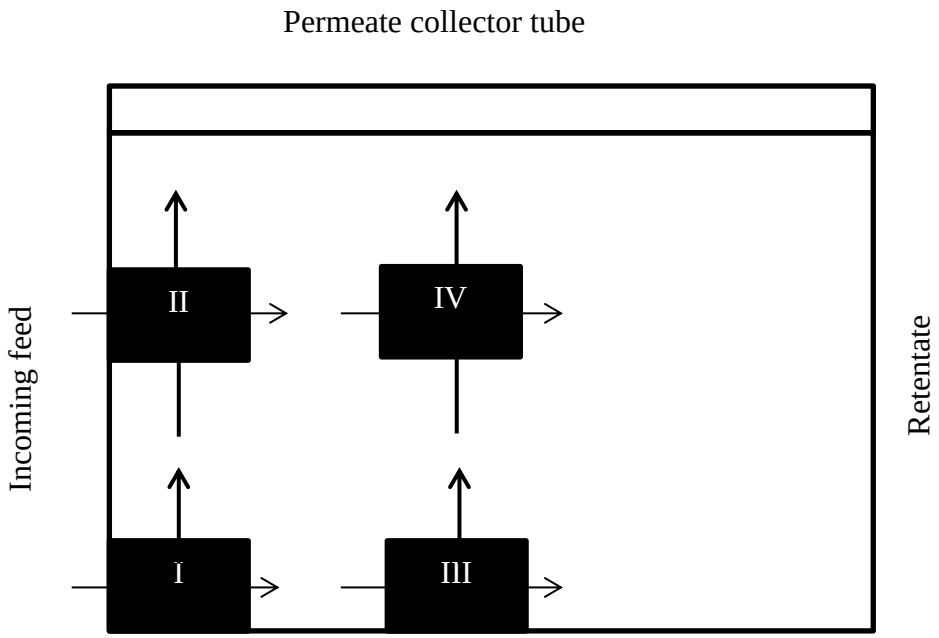

Figure 3.2: Schematic algorithm of SWM elements

In a binary mixture, the components are differentiated in term of the faster permeating component. The faster permeating component is referred as 'x_1' in the feed channel while 'y_1' in the permeate channel. The composition of permeating component for element type I and III is as follows:

$$y_1 = \frac{(\alpha-1)(\beta x_1+1)+\beta-[((\alpha-1)(\beta x_1+1)+\beta)^2-4\alpha\beta x_1(\alpha-1)]^{1/2}}{2(\alpha-1)} \quad (6)$$

where α is the selectivity of membrane and β is the pressure ratio of higher pressure side to lower pressure side. On the other hand, the flowrate into the finite element of the permeate side is given by:

$$\Delta Q = [(\frac{P_1}{\partial})(p_H x_1(i-1,1,k) - p_L y_1(i,1,k)) + (\frac{P_2}{\partial})(p_H x_2(i-1,1,k) - p_L y_2(i,1,k)]Area \quad (7)$$

where x_2=1-x_1 and y_2=1-y_1 (binary component gas mixture). The multidimensional array uses three subscripts:

- The row is represented by the first references array dimension i
- The column is represented by the second references array dimension j
- The leaf is represented by the third references array dimension k

The retentate flowrate Q_R (i, 1, k) and permeate side flow rates, Q_P (i, 1, k) contacting the next element is given by:

$$Q_P(i,1,k) = \Delta Q \quad (8)$$

$$Q_R(i,1,k) = Q_R(i-1,1,k) - \Delta Q \quad (9)$$

The feed side composition x_1 (i, 1, k) of respective element is given by:

$$x_1(i,1,k) = \frac{Q_R(i-1,1,k)x_1(i-1,1,k)-Q_P(i,1,k)y_1(i,1,k)}{Q_R(i,1,k)} \quad (10)$$

For elements in contact with feed (Type 1), the suffixes (i-1, 1, k) are replaced with feed conditions such as Q_F and x_F. These elements will not have any preceding elements in the axial direction.

For cell type II and IV elements, permeate and retentate side flowrates and compositions are known and mass transport is measured by solving the following equations:

$$\Delta Q = [(\frac{P_1}{\partial})(p_H x_1(i-1,j,k) - p_L y_1(i,j,k)) + (\frac{P_2}{\partial})(p_H x_2(i-1,j,k) - p_L y_2(i,j,k)]Area \quad (11)$$

$$\Delta Q_1 = [\left(\frac{P_1}{\partial}\right)(p_H x_1(i-1,j,k) - p_L y_1(i,j,k)]Area \quad (12)$$

$$Q_R(i,j,k) = Q_R(i-1,j,k) - \Delta Q \quad (13)$$

$$Q_P(i,j,k) = Q_P(i-1,j,k) + \Delta Q \quad (14)$$

$$x_1(i,j) = \frac{Q_R(i-1,j)x_1(i-1,j) - \Delta Q_1}{Q_R(i,j)} \quad (15)$$

$$y_1(i,j) = \frac{Q_P(i,j-1)y_1(i-1,j) - \Delta Q_1}{Q_P(i,j)} \quad (16)$$

By solving the above set of equations, the mass transport across the membrane for the entire module is computed.

3.5 Simulation Method

The separation of carbon dioxide from methane using spiral wound module is studied under variety of conditions via MATLAB. MATLAB is the high-level language and interactive environment used by millions of engineers and scientists worldwide. A user able to explore, visualize ideas and collaborate across disciplines including signal and image processing, communications, control systems, and computational finance. Sample of source code developed in MATLAB is attached in the appendices.

In order to evaluate the performance of spiral wound membrane module, the sensitivity analyses performed in the simulation are as the following:

- The effect of feed flow rate on permeate composition and permeate flow rate along length of membrane.
- The effect of feed pressure on permeate composition and permeate flow rate along length of membrane.
- The effect of number of leaf on permeate composition and permeate flow rate along length of membrane.

Table 3.1: Input parameters used for the simulation of a case study within MATLAB (S.S.M. Lock et al., 2015)

Parameters	**Value**
Permeance of CO_2 (GPU)	28.6–114.4
Permeance of CH_4 (GPU)	2.86
Feed composition	CO_2 (range between 0.1–0.6 with remaining as CH_4).
Residue CO_2 composition	< 2% (meet pipeline specification)
Feed pressure (bar)	40
Feed flow rate (SCFH)	30000-70000
Permeate pressure (bar)	1
Thickness of active membrane layer (μm)	0.1
Active length of membrane (m)	0.3-2

3.6 Gantt Chart and Key Milestones

Figure 3.3 below illustrates the timeline and the important dates in this thesis. This timeline is important in making sure the work is progressing well towards its completion**.**

No.	Details	1	2	3	4	5	6	7	8	9	10	11	12	13	14	15
1	Algorithm development															
2	Progress report submission															
3	Matlab simulation															
4	Pre-SEDEX															
5	Submission of draft report															
6	Submission of dissertation															
7	Submission of technical paper															
8	Viva oral presentation															
9	Submission of project dissertation (Hardbound)															

Figure 3.3: Gantt Chart and key milestones

Gantt Chart

Key milestones

CHAPTER 4

RESULT AND DISCUSSION

4.1 Simulation Results

Feed natural gas containing CO_2 and methane enters spiral wound module at 40 bar through an active membrane length of 3.28 ft (1m) unless specified otherwise. The permeance of CO_2 and methane are 28.6 GPU and 2.86 GPU respectively. The changes in CO_2 permeate composition radially and CO_2 retentate axially along with their flow rate are investigated and shown in the figures below. Figure 4.1 shows the composition profile of CO_2 permeate along radial direction while Figure 4.2 illustrates the flow rate profile of permeate along radial length. The simulation result shows that the composition of CO_2 permeate decrease slightly and keep constant after certain radial length. Theoretically, the composition of CO_2 permeate will increase due to more CO_2 permeation along radial direction, however the increase in permeate flow rate as shown in Figure 4.2 is more significant, which results in the dilution of CO_2 permeate.

Figure 4.3 shows the composition profile of CO_2 retentate in axial direction while Figure 4.4 indicates the flow rate profile of retentate in axial direction. The compostion of CO_2 retentant decrease steadily along axial direction due to the permeation of CO_2 into permeate stream (Qi and Henson, 1996). The same profile trend can be seen in the flow rate of retentate along axial direction. As the permeation progress, the amount of CO_2 leaving retentate stream into permeate stream increase and hence resulting in less flow rate in retentate stream.

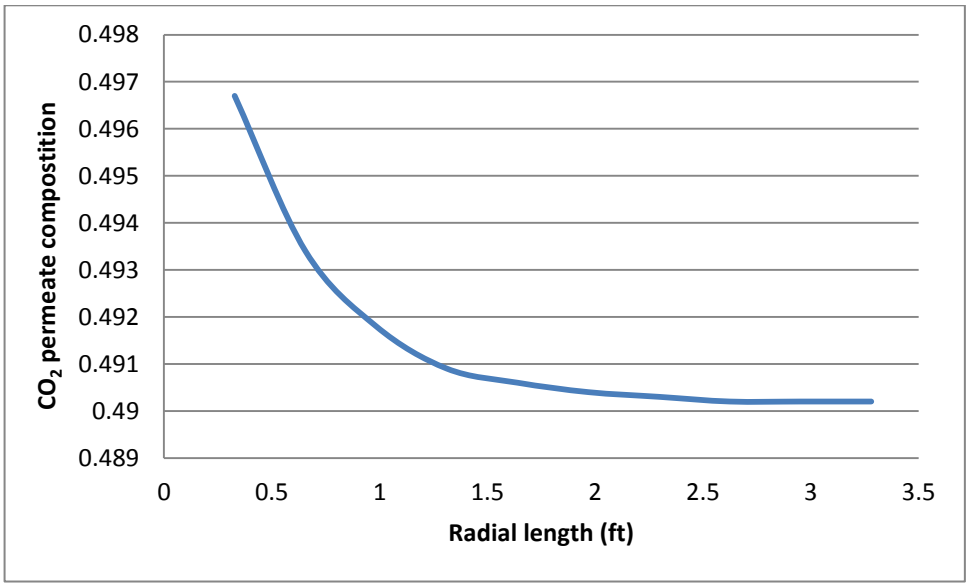

Figure 4.1: CO_2 permeate composition profile in radial direction

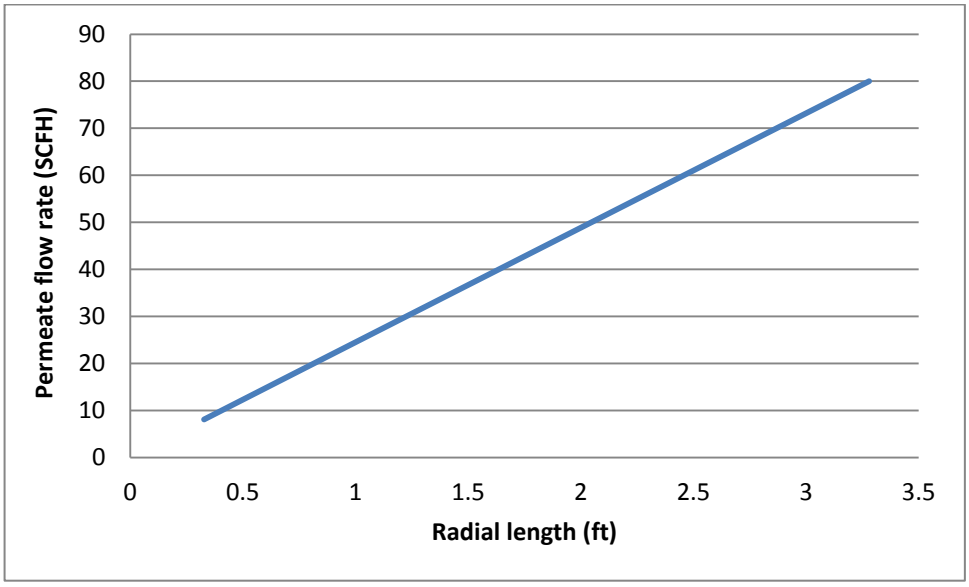

Figure 4.2: Permeate flow rate profile in radial direction

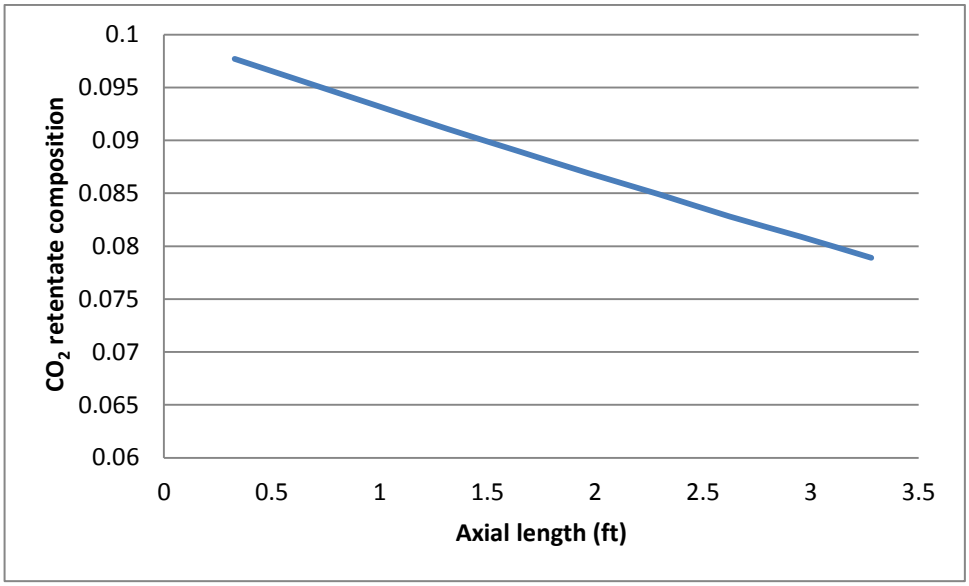

Figure 4.3: CO_2 retentate composition profile in axial direction

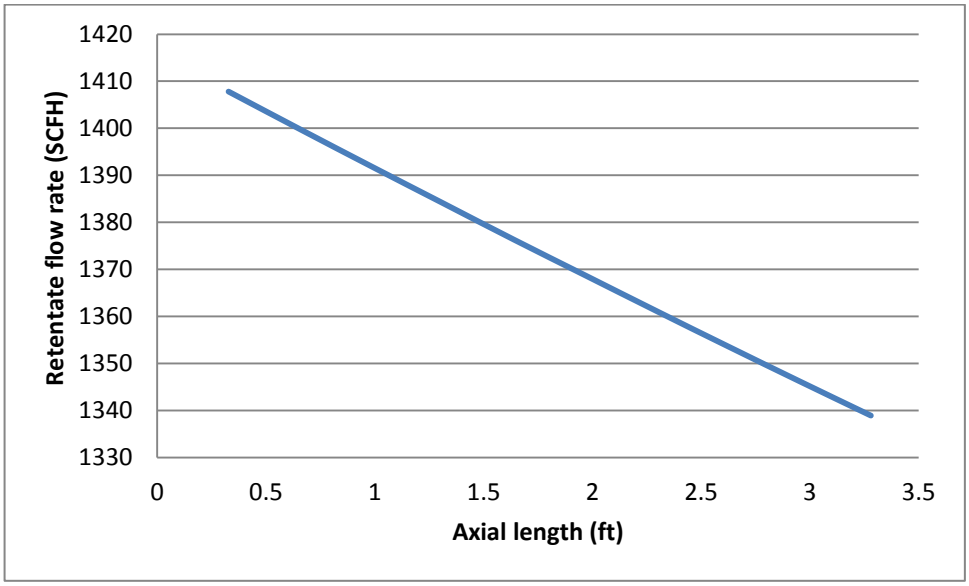

Figure 4.4: Retentate flow rate profile in axial direction

4.2 Model validation

Model validation is important to demonstrate the accuracy of the simulation model. In this study, the model is validated using published experimental data by Qi and Henson (1996) for their respective binary gas (CO_2/CH_4) separation system. The parameters used as input for computation of the simulation model for validation is presented in Table 4.1.

Table 4.1: Experiment data from Qi and Henson (1996)

Data set	**Measurement**				
	Q_f (m^3/s)	P (MPa)	x_f	θ	y_p
1	0.0331	3.7557	0.0523	0.3762	0.1318
2	0.0318	2.3767	0.0528	0.2887	0.1564
3	0.0331	3.8247	0.1161	0.4059	0.2676
4	0.0466	3.2041	0.1213	0.3310	0.3345
5	0.0695	4.8589	0.1234	0.3538	0.3319
6	0.0692	3.9626	0.1241	0.2796	0.3732
7	0.0370	3.2386	0.1272	0.3628	0.3212
8	0.0774	4.8589	0.1298	0.3051	0.3766
9	0.0672	3.8936	0.1339	0.2537	0.4081
10	0.0367	3.8936	0.2134	0.5000	0.4115

The results are tabulated and plotted in line graph. Fig. 4.5 compares the CO_2 permeate composition while Fig. 4.6 compares the stage cut of the simulation result with experiment data. Stage cut is calculated as:

$$Stage\ cut = \frac{Permeate\ flow\ rate, Q_p}{Feed\ flow\ rate, Q_F}$$

Fig. 4.5 and Fig 4.6 suggested that the simulation give good approximation to the published experiment data. In overall, the percentage errors are less than 10 percent.

Table 4.2: Comparison of experiment data and simulation result for CO_2 permeate composition, y_p

Data set	Measurement					
	Q_f (m^3/s)	P (MPa)	x_f	y_p (experiment)	y_p (simulation)	**Error (%)**
1	0.0331	3.7557	0.0523	0.1318	0.13530	2.65
2	0.0318	2.3767	0.0528	0.1564	0.16403	4.87
3	0.0331	3.8247	0.1161	0.2676	0.25630	4.22
4	0.0466	3.2041	0.1213	0.3345	0.32530	2.75
5	0.0695	4.8589	0.1234	0.3319	0.31824	4.11
6	0.0692	3.9626	0.1241	0.3732	0.36913	1.09
7	0.0370	3.2386	0.1272	0.3212	0.34940	8.77
8	0.0774	4.8589	0.1298	0.3766	0.35686	5.24
9	0.0672	3.8936	0.1339	0.4081	0.38601	5.41
10	0.0367	3.8936	0.2134	0.4115	0.44620	8.43

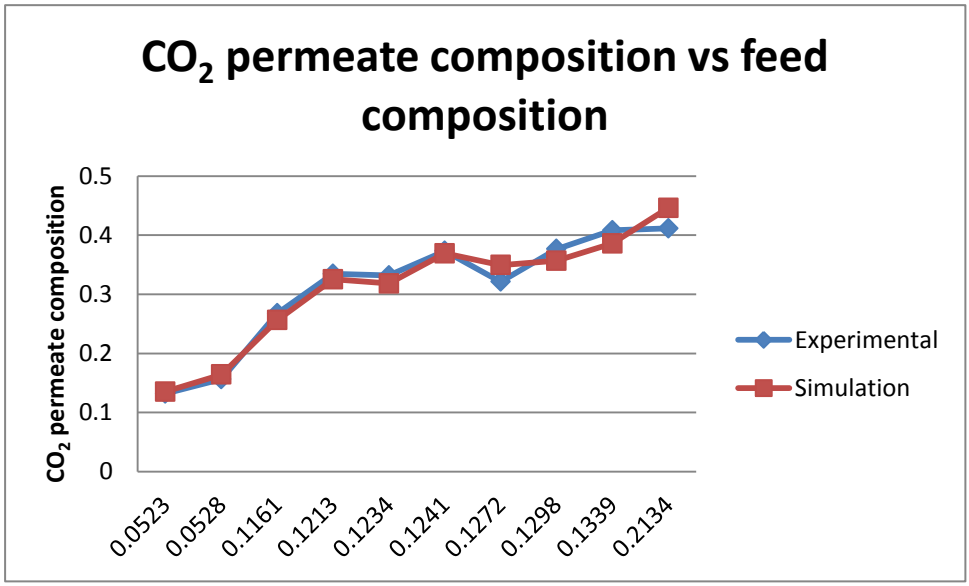

Figure 4.5: Model validation with published experimental data of CO_2 permeate composition

Table 4.3: Comparison of experiment data and simulation result for stage cut

Data set	**Measurement**					
	Q_f (m^3/s)	P (MPa)	x_f	Stage cut, θ (experiment)	Stage cut, θ (simulation)	**Error (%)**
1	0.0331	3.7557	0.0523	0.3762	0.3947	4.91
2	0.0318	2.3767	0.0528	0.2887	0.2748	4.81
3	0.0331	3.8247	0.1161	0.4059	0.4235	4.33
4	0.0466	3.2041	0.1213	0.331	0.3164	4.41
5	0.0695	4.8589	0.1234	0.3538	0.3207	9.35
6	0.0692	3.9626	0.1241	0.2796	0.2643	5.47
7	0.0370	3.2386	0.1272	0.3628	0.3569	1.62
8	0.0774	4.8589	0.1298	0.3051	0.2878	5.67
9	0.0672	3.8936	0.1339	0.2537	0.2735	7.80
10	0.0367	3.8936	0.2134	0.5000	0.5113	2.26

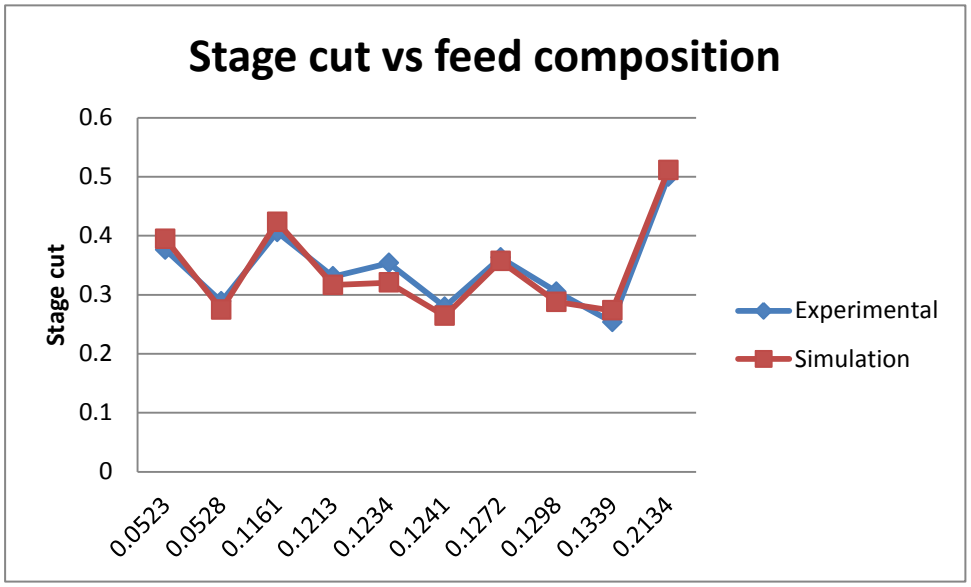

Figure 4.6: Model validation with published experimental data of stage cut

4.3 The Effect of Feed Flow Rate

The simulation is performed by varying the feed flow rate while other parameters are maintained. Starting from 30000 SCFH, the feed flow rate is increased by 10000 SCFH until it reaches 70000 SCFH.

Figure 4.7 shows the composition profile of CO_2 permeate composition along active membrane length for different feed flow rate. On the other hand, Figure 4.8 shows the flow rate of permeate along active membrane length. The results indicate that higher feed flow rate leads to higher CO_2 permeate composition and permeate flow rate (Chowdury, 2011). Higher feed flow rate promote turbulent flow in feed spacer, hence resulting in more permeation passes through membrane sheet.

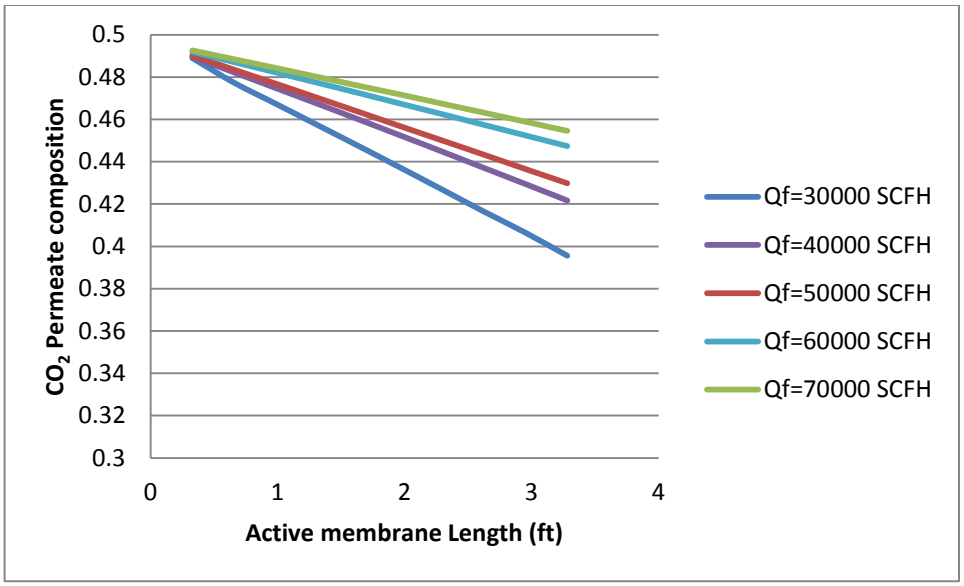

Figure 4.7: Effect of feed flow rate on CO_2 permeate composition along active membrane length

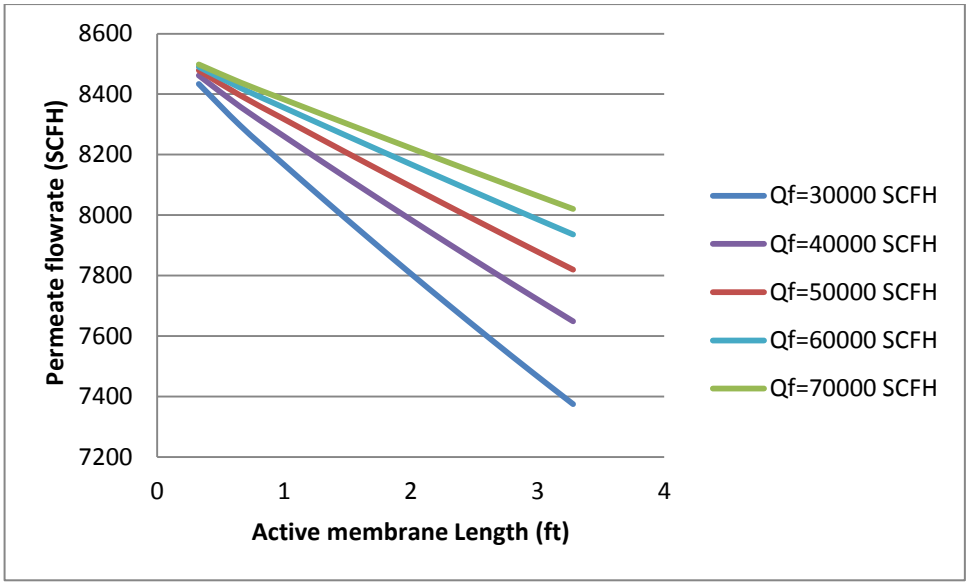

Figure 4.8: Effect of feed flow rate on permeate flow rate along active membrane length

4.4 The Effect of Feed Pressure

The simulation is performed by varying the feed pressure in order to study the effect towards CO_2 permeate composition and flow rate. The feed pressure starts at 30 bar and increases by 10 bar until 60 bar.

Figure 4.9 shows the CO_2 permeate composition along active membrane length while Figure 4.10 indicates the permeate flow rate. Based on Figure 4.6, 60 bar of feed pressure results in the highest composition of CO_2 permeate initially but decrease significantly along the active membrane length. This indicates that most of CO_2 permeation for 60 bar feed pressure occurs in the early length of active membrane. Hence, the next subsequent cell along the membrane length receives less input of CO_2 composition which explain the significant drop in CO_2 permeate composition towards the end of membrane length. On the other hand, the composition of CO_2 permeate at 20 bar started at the lowest value compared to other pressure but decrease very steadily towards the end. The results demonstrate that high pressure promote more permeation as pressure is the main driving force in membrane gas separation (J.G.A. Bitter, 1991). Meanwhile, Figure 4.10 indicates that higher feed pressure promote more permeate flow rate because of the more permeation progress.

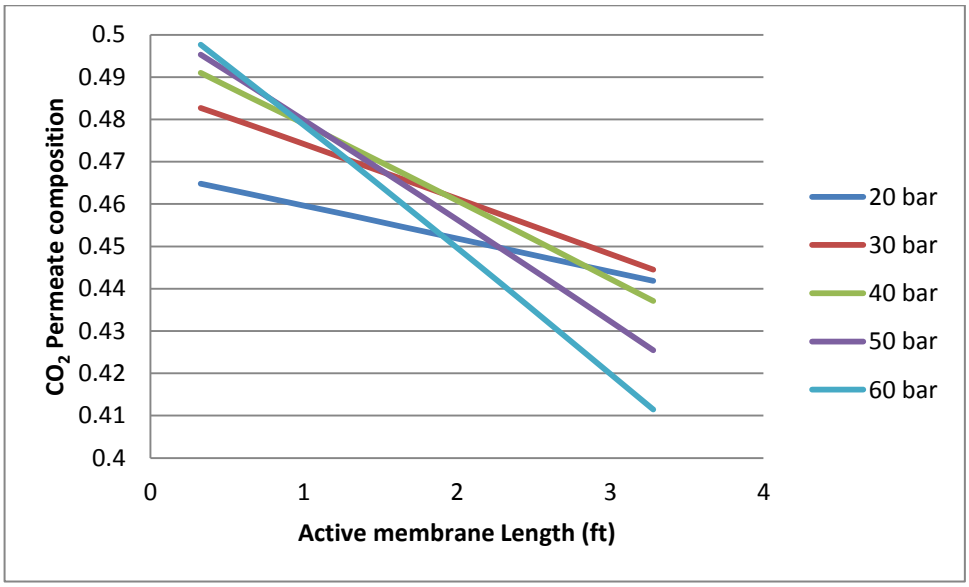

Figure 4.9: Effect of feed pressure on CO_2 permeate composition along active membrane length

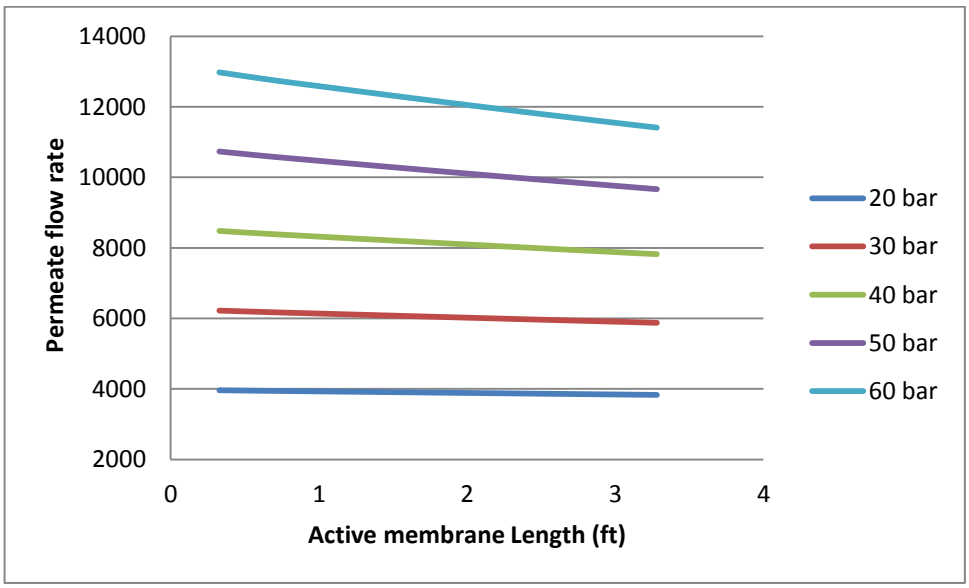

Figure 4.10: Effect of feed pressure on permeate flow rate along active membrane length

4.5 The Effect of Membrane Leaf Number

The simulation is done by varying the number of membrane leaf. Starting with 4 leaf, the number of leaf is increased by 5 until 20 leaf. Figure 4.11 shows the CO_2 permeate composition along active membrane length while Figure 4.12 indicates the permeate flow rate.

Based on Figure 4.12, it can be noticed that the more number of leaf promote more separation. Membrane separation depends strongly on the mass transfer area per volume. Generally, the more membrane leaf packed into a spiral wound module, the higher mass transfer area per volume and its packing density (Marriot et al., 2001). On the other hand, Figure 4.11 demonstrates that the changes in composition for different number of leaf are quite the same because every membrane leaf has its own permeate spacer. For the same feed conditions and membrane parameters, the permeation for every leaf is more or less the same. Hence, the higher number of membrane leaf able to promote more separation.

.

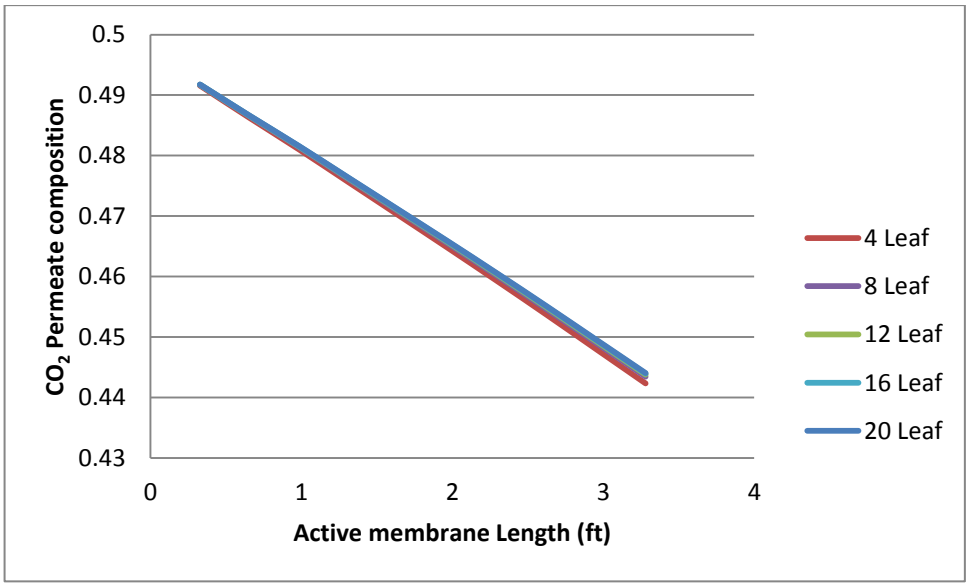

Figure 4.11: Effect of number of leaf on CO_2 permeate composition along active membrane length

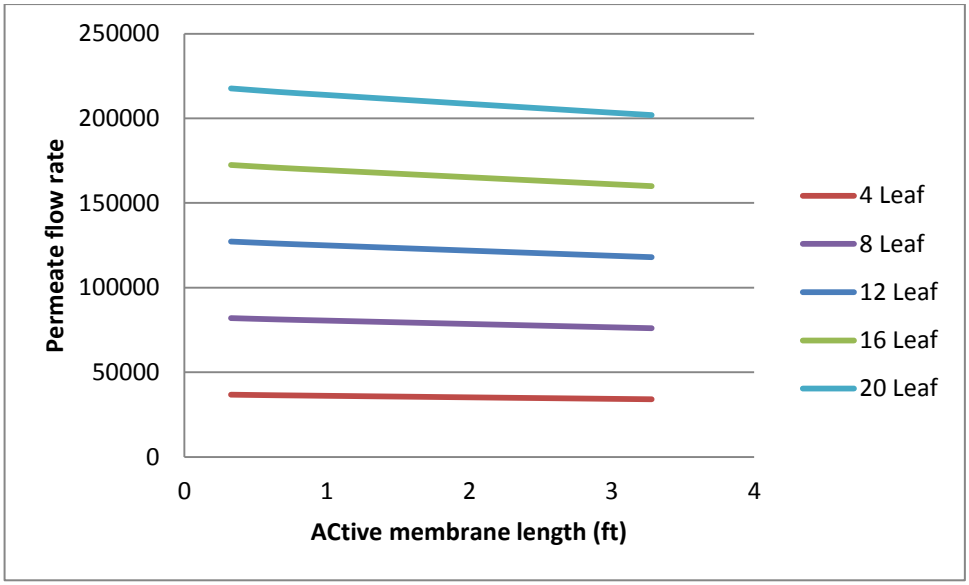

Figure 4.12: Effect of number of leaf on permeate flow rate along active membrane length

CHAPTER 5

CONCLUSION AND RECOMMENDATION

5.1 Conclusion

As a conclusion, this thesis managed to model spiral wound membrane module for CO_2 capture from natural gas. Regarding the first objective of this thesis, a mathematical model has been developed to simulate the CO_2 capture from natural gas using spiral wound membrane module. Approaching the problem using succession of state method is shown to be an effective approach for the membrane module modeling. However, the real advantage of this method has not been implemented here which is the incorporation of concentration, pressure and temperature dependent permeability.

The composition profiles of CO_2 in the permeate and retentate stream along with their flow rate have been illustrated in the simulation results using MATLAB. On the other hand, for the sensitivity analysis which is the second objective, some factors which affecting the spiral wound membrane module separation performance are investigated. The effect of feed flow rate and feed pressure on permeate stream has been studied. Generally, the higher feed flow rate and feed pressure promote more separation for spiral wound module. Moreover, the number of membrane leaf is proved to significantly improve the separation of CO_2 from natural gas using spiral wound module.

5.2 Recommendation

Pressure drop may have significant effect in the feed spacer of spiral wound membrane module due to the turbulent flow. Hence, future work should include the effect of pressure drop in the mathematical model. Furthermore, the variation of channel height may be investigated because it affects the active membrane area and packing density. High channel height can cause less mass transfer area but able to minimize the pressure drop across the feed spacer while low channel height results to high pressure drop but enable more mass transfer area to be packed in a spiral wound membrane (E. Drioli et al., 2011).

REFERENCES

Ahmad, A.L., Leo, C.P., Shukor, S.R. (2008). Preparation of silica/c-alumina membrane with bimodal porous layer for improved permeation in ions separation. *Journal of American Ceramic Society, 91*, 2009–2014.

Armaroli, N., Balzani, V. (2011). *Energy for a Sustainable World: From the Oil Age to a Sun-Powered Future*. WILEY-VCH Verlag GmbH & Co. KGaA, Weinheim.

Baker, R.W., Lokhandwala, K. (2008). Natural gas processing with membranes. An overview. *Industrial and Engineering Chemistry Research, 47*, 2109–2121.

Brouckaert C.J. and Buckley C.A. Simulation of tubular reverse osmosis. *Water SA, 18*(3), 215-224, 1992.

Cao, C., Wang, R., Chung, T.S., Liu, Y. (2002). Formation of high-performance 6FDA-2,6- DAT asymmetric composite hollow fiber membranes for CO_2/CH_4 separation. *Journal of Membrane Science. 209*, 309–319.

Chern, R.T., W.J. Koros and P.S. Fedkiw (1985). Simulation of a hollow-fiber gas separator: the effects of process and design variables. *Ind. Eng. Chem. Process Des. Dev., 24*, 1015.

Chew, T.-L., Ahmad, A.L., Bhatia, S. (2010). Ordered mesoporous silica (OMS) as an adsorbent and membrane for separation of carbon dioxide (CO_2). *Advances in Colloid and Interface Science, 153*, 43–57.

Coker, D.T., B.D. Freeman and G.K. Fleming (1998). Modeling multicomponent gas separation using hollow-fiber membrane contactors. *AIChE J., 44*, 1289.

E. Drioli et al. (2011). *Membrane Engineering for the Treatment of Gases: Gas-Separation Problems with Membranes*. Royal Society of Chemistry.

Faizan, A., Lau, K.,K., Lock, S., S., M., Sikender, R., Asad, U., K., Lee, M. (2014). Hollow fiber membrane model for gas separation: Process simulation, experimental validation and module characteristics study. *Journal of Industrial and Engineering Chemistry, 21*, 1246–1257.

IPCC (2007). Intergovernmental Panel on: Climate Change 2007: The Physical Science Bases Contribution of Working Group 1 to the Fourth Assessment *Report of the Intergovernmental Panel on Climate Change Series*. Cambridge University Press, Cambridge, United Kingdom and NewYork, USA.

J.G.A. Bitter, (1991). *Transport Mechanisms in Membrane Separation Processes.* New York: Plenum Press.

J. Johnson, M. Busch (2010). Engineering aspects of reverse osmosis module design. *Desalination and Water Treatment, 15* (1–3), 236–248.

Kidnay, A.J., Parrish, W.R., McCartney, D.G. (2011). *Fundamentals of Natural Gas Processing.* Boca Raton: Taylor & Francis Group.

Marriott, J.I., E. Sørensen and I.D.L. Bogle (2001). Detailed mathematical modeling of membrane modules. *Computers Chem. Engng., 25,* 693.

Meindersma, G., Kuczynski, M. (1996). Implementing membrane technology in the process industry: problems and opportunities. *Journal of Membrane Science, 113*, 285–292.

Merkel, T.C., Gupta, R., Turk, B.F. (2001). Mixed-gas permeation of syngas components in poly(dimethylsiloxane) and poly(1-trimethylsilyl-1-propyne) at elevated temperatures. *Journal of Membrane Science, 191*, 85–94.

M. H. M. Chowdury (2011). *Simulation, Design and Optimization of Membrane Gas Separation, Chemical Absorption and Hybrid Processes for CO_2 Capture*. University of Waterloo, Canada.

Miki, Y., Kenji, H. (2010). *CO_2/CH_4 Mixed Gas Separation Using Carbon Hollow Fiber Membranes*. Energy Procedia 37, 1109–1116.

M. J. Thundyil, W. J. Koros (1997). Mathematical modeling of gas separation permeators—for radial crossflow, countercurrent, and concurrent hollow fiber membrane modules, *Journal Membrane Science, 125*, 275–291.

Mokhatab, S., Poe, W.A., Speight, J.G. (2006). *Handbook of Natural Gas Transmission and Processing*. Oxford: Gulf Professional Publishing.

Mulder M.H.V. (1996). *Basic Principles of Membrane Technology*. The Netherland: Kluwer Academic Publishers.

Narinsky A.G. (1991). Applicability conditions of idealized flow models for gas separations by asymmetric membrane. *Journal of Membrane Science, 55*, 333-347.

Ng, B.C., Ismail, A.F., Abdul Rahman, W.A., Hasbullah, H., Abdullah, M.S., Hassan, A.R. (2004). Formation of asymmetric polysulfone flat sheet membrane for gas separation: rheological assessment. *Jurnal of Teknologi, 41*, 73–88.

Nord, L.O., Anantharaman, R., Bolland, O. (2009). Design and off-design analyses of a pre- combustion CO_2 capture process in a natural gas combined cycle power plant. *International Journal of Greenhouse Gas Control, 3,* 385–392.

Ohlrogge, K., Wind, J., Brinkmann, T. (2002). *Membrane Technology for Natural Gas Processing*. Calgar: SPE Gas Technology Symposium.

Pan, C.Y. (1983). Gas separation by permeators with high flux asymmetric membranes. *AIChE J., 29,* 546.

Ren, J., Chung, T.S., Li, D., Wang, R., Liu, Y. (2002). Development of asymmetric 6FDA- 2,6DAT hollow fiber membranes for CO_2/CH_4 separation 1. The influence of dope composition and rheology on membrane morphology and separation performance. *Journal of Membrane Science, 207*, 227–240.

Runhong, Q., Michael, A., H. (1996). Optimal design of spiral-wound membrane networks for gas separations. *Journal of Membrane Science, 148*, 71–89.

Schoots, K., Rivera-Tinocoa, R., Verbongb, G., van der Zwaan, B. (2011). Historical variation in the capital costs of natural gas, carbon dioxide and hydrogen pipelines and implications for future infrastructure. *International Journal of Greenhouse Gas Control, 5*, 1614–1623.

Shao, P., Dal-Cin, M.M., Guiver, M.D., Kumar, A. (2013). Simulation of membrane based CO_2 capture in a coal-fired power plant. *Journal of Membrane Science, 427*, 451–459.

Speight, J.G. (2007). *Natural Gas: A Basic Handbook*. Houston: Gulf Publishing Company.

S. S. M. Lock et al. (2015). Modeling, simulation and economic analysis of CO2 capture from natural gas using cocurrent, countercurrent and radial crossflow hollow fiber membrane. *International Journal of Greenhouse Gas Control, 36*, 114-134.

Thundyil, M.J., and W.J. Koros (1997). Mathematical modeling of gas separation permeators – for radial crossflow, countercurrent, and cocurrent hollow fiber membrane modules. *Journal Membrane Science, 125,* 275.

Wang, R., S.L. Liu, T.T. Lin and T.S. Chung (2002). Characterization of hollow fiber membranes in a permeator using binary gas mixtures. *Chemical Engineering Science, 57*, 967.

Xiao, Y., Low, B.T., Hosseini, S.S., Chung, T.S., Paul, D.R. (2009). The strategies

of molecular architecture and modification of polyimide-based membranes for CO_2 removal from natural gas—a review. Progress in Polymer Science 34, 561–580.

Zhao, J., Wang, Z., Wang, J., Wang, S. (2006). Influence of heat-treatment on CO_2 separation performance of novel fixed carrier composite membranes prepared by interfacial polymerization. *Journal of Membrane Science, 283*, 346–356.

APPENDICES

a. Example of Source Code in MATLAB

```
A = input ('please enter no of row cell > ');
C = input ('please enter no of column cell > ');
num_rows=[A,A];
num_cols=[C,C];
k = input ('please enter the number of leaf, minimum number of leaf
is 2 > ');
num_leaf=k;
P1=0.0000286;%permeability of co2
P2=0.00000286;%permeability of ch4
a=P1/P2;
area=0.01;%active area of cell
d=0.00000025;%thickness active layer on membrane
pL=1;%low pressure
pH=40;%high pressure
B=pH/pL;%constant value
y=zeros(A,C,k);
Q=zeros(A,C,k);
Qp=zeros(A,C,k);
Qr=zeros(A,C,k);
Q1=zeros(A,C,k);
x=zeros(A,C,k);
xf=0.1;
Qf=1415.84;
for k=1:1:num_leaf
    for i=1:1:num_rows
        for j=1:1:num_cols
         if i==1 && j ==1 && k==1
            y(1,1,k)=((a-1)*(B*xf + 1) + B - sqrt(((a-1)*(B*xf + 1)
+ B)^2 - 4*a*B*xf*(a-1)))/(2*(a-1));
            Q(1,1,k)=((P1/d)*(pH*xf-pL*y(1,1,k)) + (P2/d)*(pH*(1-
xf)-pL*(1-y(1,1,k))))*area;
            Qp(1,1,k)=Q(1,1,k);
            Qr(1,1,k)=Qf-Q(1,1,k);
            x(1,1,k)=(Qf*xf-Qp(1,1,k)*y(1,1,k))/Qr(1,1,k);
         elseif j==1 && i>1
            y(i,1,1)=((a-1)*(B*x(i-1,1,1) + 1) + B - sqrt(((a-
1)*(B*x(i-1,1,1) + 1) + B)^2 - 4*a*B*x(i-1,1,1)*(a-1)))/(2*(a-1));
            Q(i,1,1)=((P1/d)*(pH*x(i-1,1,1)-pL*y(i,1,1)) +
(P2/d)*(pH*(1-x(i-1,1,1))-pL*(1-y(i,1,1))))*area;
            Qp(i,1,1)=Q(i,1,1);
            Qr(i,1,1)=Qr(i-1,1,1)-Q(i,1,1);
            x(i,1,1)=(Qr(i-1,1,1)*x(i-1,1,1)-
Qp(i,1,1)*y(i,1,1))/Qr(i,1,1);
         elseif i==1 && j>1
            y(1,j,1)=((a-1)*(B*((xf+x(i,j-1,1))/2) + 1) + B -
sqrt(((a-1)*(B*((xf+x(i,j-1,1))/2) + 1) + B)^2 - 4*a*B*((xf+x(i,j-
1,1))/2)*(a-1)))/(2*(a-1));
            Q(1,j,1)=((P1/d)*(pH*((xf+x(i,j-1,1))/2)-pL*y(1,j,1)) +
(P2/d)*(pH*(1-((xf+x(i,j-1,1))/2))-pL*(1-y(1,j,1))))*area;
            Q1(1,j,1)=(P1/d)*(pH*((xf+x(i,j-1,1))/2)-
pL*y(1,j,1))*area;
            Qp(1,j,1)=Qp(1,j-1,1)+Q(1,j,1);
            Qr(1,j,1)=Qf-Q(1,j,1);
            x(1,j,1)=(Qf*((xf+x(i,j-1,1))/2)-Q1(1,j,1))/Qr(1,j,1);
         end
```